IGARSS 2020 - 2020 IEEE International Geoscience and Remote Sensing Symposium | 978-1-7281-6374-1/20/$31.00 ©2020 IEEE | DOI: 10.1109/IGARSS39084.2020.9324404

INVESTIGATING THE IMPACT OF COHERENT AND INCOHERENT SCATTERING TERMS IN GNSS-R DELAY DOPPLER MAPS

Hugo Carreno-Luengo[1], Chris Ruf[1], April Warnock[2], and Kelsey Brunner[2]

[1]Climate and Space Sciences and Engineering Department, University of Michigan (UM)
[2]SRI International
Ann Arbor, MI, United States of America (USA)
Email: {carreno,cruf}@umich.edu, {april.warnock,kelsey.brunner}@sri.com

ABSTRACT

Forward scattering properties of Earth-reflected Global Navigation Satellite Systems (GNSS) signals are evaluated over land surfaces. The CYclone Global Navigation Satellite System (CYGNSS) End-to-End Simulator (E2ES) is updated. A GNSS-Reflectometry (GNSS-R) model capable of evaluating both the incoherent and the coherent scattering terms is developed based on the Huygens-Kirchhoff principle. The coherent term is studied for incidence angles $\theta_i \sim$ [0, 80]° over a wide range of surface height standard deviation σ = [1, 4] cm and Vegetation Optical Depth VOD = [0, 1.5]. This model is validated over a lake with space-borne data as generated using the CYGNSS raw IF processor. Results demonstrate the impact of higher order Fresnel zones on the spatial resolution of GNSS-R over heterogenous areas, showing "ringing" fluctuations in the reflected power near high contrast boundaries. We expect to contribute to the accurate interpretation of datasets over inland water bodies.

Index Terms— GNSS-R, CYGNSS, coherent and incoherent scattering, aperture diffraction theory, Huygens-Kirchhoff, Fresnel zones, inland water bodies, vegetation

1. INTRODUCTION

GNSS-R is a type of L-band passive multi-bistatic radar, with as many transmitters as navigation spacecrafts are in view. It provides global coverage, full temporal availability, and sampling of the Earth's surface over multiple tracks simultaneously within a wide area up to ~ 1,500 km. The use of GNSS radio-navigation signals for Earth remote sensing has been investigated since they were originally proposed for mesoscale ocean altimetry by the European Space Agency (ESA) in 1993 [1,2]. The first feasibility study from space corresponds to an experiment performed at the Jet Propulsion Laboratory (JPL) using the Space-borne Imaging Radar-C (SIR-C) on-board the Space Shuttle [3]. This experiment pushed forward the development of GNSS-R from small satellites such as e.g. CubeSats [4]. Several feasibility studies have been performed from several platforms, including United Kingdom (U.K.) Disaster Monitoring System-1 (DMC-1) [5], U.K. TechDemoSat-1 (TDS-1) [6], and Soil Moisture Active Passive (SMAP) [7].

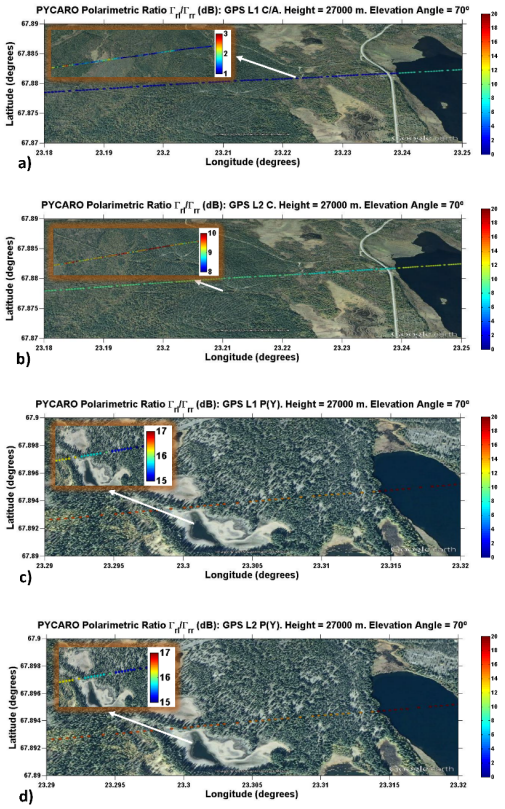

Fig. 1. Sensitivity of the Polarimetric Ratio to inland water bodies and boreal forests from an ESA-sponsored stratospheric balloon experiment performed in October 2014 [4]. PYCARO instrument [4,12] collected strong coherent Earth-reflected GNSS signals from an altitude up to ~ 27 km.

In 2012, the National Aeronautics and Space Administration (NASA) selected the CYGNSS mission led by the University of Michigan (UM) as a low cost and high science Earth Venture Space System [8-11]. CYGNSS, an eight-microsatellite fully operational constellation, was launched on December 15th, 2016 into a Low Earth Orbit (LEO) with an inclination angle ~ 35°. The main objective of this mission is to estimate wind speed over tropical cyclones with an unprecedented spatio-temporal sampling of the ocean [8].

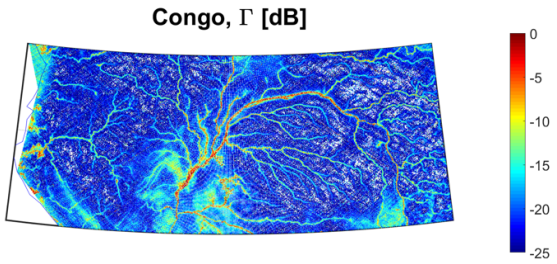

Fig. 2. CYGNSS-derived [9] reflectivity Γ over Congo rainforests. Small inland water bodies are detected even with very high Above-Ground Biomass (AGB) up to ~ 500 ton/ha [17].

The first GNSS-R studies assumed the scattered electric field E_s to be totally incoherent. More recently, some studies [4,12,13] have demonstrated that there is also a non-negligible coherent scattering term, especially in the presence of calm inland water bodies (Fig. 1). The coherent scattering area is usually defined by rule of thumb as the first Fresnel zone. This point was revised in [14], showing that contributions from higher order Fresnel zones also affect the total received power.

While scattering from large smooth regions is well understood, it remains uncertain how to model the composite scattering from smaller smooth regions interspersed within a larger rough terrain [15-19]. The surface properties, i.e. topographic roughness and small scale surface roughness, shall be considered for an accurate analysis over rough land surfaces in the presence of small water bodies [17]. In this work, we investigate in detail the scattering properties over inland water bodies, including the impact of vegetation, and surface roughness (Fig. 2). This paper is organized as follows. Section 2 describes the GNSS-R model. The results are presented and described in Section 3. The CYGNSS E2ES "coherent module" is presented in Section 4. Conclusions are included in Section 5.

2. COHERENT AND INCOHERENT SCATTERING GNSS-R MODEL

Electromagnetic wave scattering from an extended surface may be treated as a problem in aperture diffraction theory if the reflected field at a clear aperture plane of the surface can be determined as a function of the source field which is incident on the surface. The foundation of aperture diffraction theory starts with the vector equivalent Helmholtz integral.

Here, we apply the Huygens-Kirchhoff principle to relate the statistics of the reflected signals to the statistics of an irregular surface. In this scenario, the scattered electric field E_s from the Earth surface due to an spherical incident wave is given by:

$$E_s = -j\iint \frac{E(\bar{\rho})\bar{n}\bar{q}}{4\pi R_t(\bar{\rho})R_r(\bar{\rho})} e^{jk(R_t(\bar{\rho})+R_r(\bar{\rho}))} dA \qquad (1)$$

where $\bar{n}$ is the unit vector normal to the surface at the specular point, $\bar{q}$ is the scattering vector, k is the angular wavenumber, R_r and R_t are, respectively, the ranges from the transmitter and the receiver to the specular reflection point, A is the scattering area, and $\bar{\rho}$ is the positioning vector of the scattering point. Under the assumption of small surface slopes, we can further approximate:

$$\bar{n}\bar{q} \approx -kz(R_t - R_r) \approx k(\cos\theta_{i,i} + \cos\theta_{i,s}) \qquad (2)$$

where z is the vertical coordinate, $\theta_{i,i}$ and $\theta_{i,s}$ are the incidence angle of the incident and the reflected signal. In the specular direction, it can be assumed that:

$$\theta_{i,i} = \theta_{i,s} = \theta_i \qquad (3)$$

Finally, E is defined as it follows:

$$E = \sqrt{\gamma |R(\bar{\rho}))|^2 e^{-(2k\sigma(\bar{\rho})\cos\theta_i)^2}} \qquad (4)$$

where γ is the transmissivity of the vegetation, R is the complex Fresnel reflection coefficient, and σ is the surface height standard deviation (related to small-scale surface roughness). The transmissivity of the vegetation can be estimated as:

$$\gamma = e^{-2VOD(\bar{\rho})/\cos\theta_i} \qquad (5)$$

where VOD is the Vegetation Optical Depth. VOD is an index of leaf and woody biomass that is used to parameterize absorption effects.

As such, in a GNSS-R scenario like that of the CYGNSS mission:

$$E_s = -jk\iint \frac{2E(\bar{\rho})\cos\theta_i}{4\pi R_t(\bar{\rho})R_r(\bar{\rho})} e^{jk(R_t(\bar{\rho})+R_r(\bar{\rho}))} dA \qquad (6)$$

The reflected power can be derived as:

$$P_s = \upsilon P_t G_t \frac{\lambda^2 G_r}{4\pi} |E_s|^2 \qquad (7)$$

where υ is the characteristic free space wave impedance ~ 120π, P_t is the power of the transmitted Global Positioning System (GPS) signals, G_t is the gain of the transmiting antenna, G_r is the gain of the receiving antenna, and λ is the signal wavelength.

Finally, power Delay Doppler Maps (DDMs) can be generated as a 2-Dimensional convolution product:

$$\langle |Y(\tau,f)|^2 \rangle \approx P_s(\tau,f) ** |X(\tau,f)|^2 \qquad (8)$$

where X is the so-called Woodward Ambiguity Function (WAF). It can be approximated as it follows:

$$X(\tau,f) \approx \Lambda(\tau - (R_t + R_t)/c) S(f_D - f_c) \qquad (9)$$

where Λ is the Pseudo-Random-Noise (PRN) code autocorrelation function representing the impulse response of the system in the time domain, S is the sinc-exponential function, τ is the delay of the signal from the transmitter to the receiver, f_D is the Doppler shift of the reflected signal, f_c is aimed to compensate the Doppler shift of the signal, and c is the speed of light.

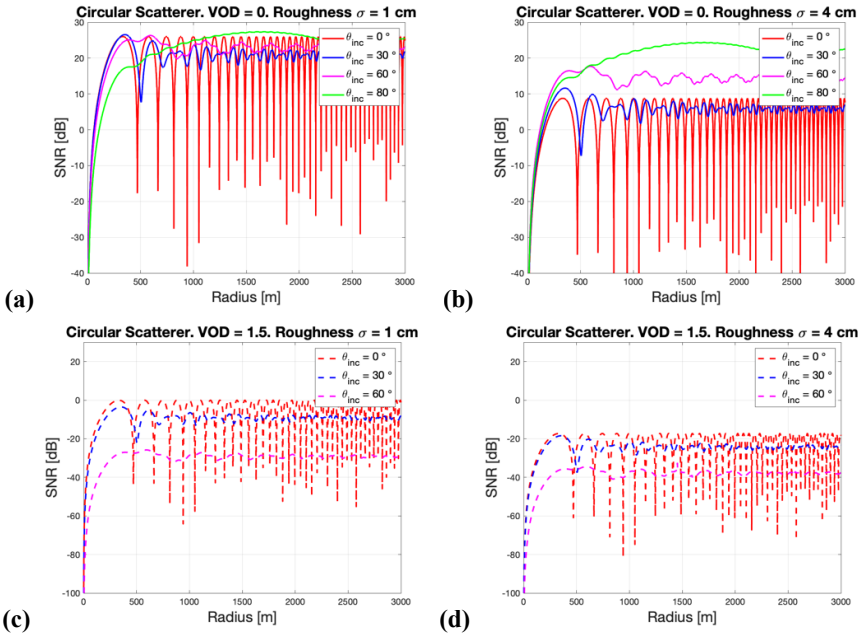

Fig. 3. Simulated Signal-to-Noise Ratio (SNR) of the coherent scattering term as a function of the radius of a circular scatterer. Impact of attenuation is evaluated through the Vegetation Optical Depth: (a),(b) VOD = 0; (c),(d) VOD = 1.5. Impact of surface roughness is evaluated through the surface height standard deviation: (a),(c) σ = 1 cm; (b),(d) σ = 4 cm. The results are evaluated as a function of the incidence angle. Grazing angles are out of scale in (c),(d). The modulus of the Fresnel reflection coefficient is equal to 1.

The Huygens-Kirchhoff approximation was selected in this work. This approximation has been previously shown to produce relatively consistent results using two different approaches [20]: 1) numerically solving the Helmholtz integral equations, and 2) using a Monte Carlo method under the Huygens-Kirchhoff approximation. These approaches can be implemented using finite length surface segments and a tapering function to avoid edge effects. This implementation (as opposed to periodic surfaces) is more convenient for comparision with approximate theoretical methods applied to randomly rough surfaces.

3. PRELIMINARY RESULTS: COHERENT SCATTERING OVER INLAND WATER BODIES

In this section, the coherent scattering term is evaluated over inland water bodies using the previous GNSS-R model. Theoretically, the integral in Eqn. (8) extends over an infinite surface. This is valid when a large number of complete Fresnel zones take part in the re-radiation from the surface. In practice, this approximation is not valid because the contributions of the scatterers decrease quickly as they get farther away from the nominal specular reflection point. In this work, the domain of the discrete scattering integral was an area of 20 km x 20 km. A circular scatterer with a Fresnel reflection coefficient equal to 1 was set in the center to reproduce a "synthetic" lake surface. The integration step was set to 1 m.

3.1 Impact of Multiple Fresnel Zones

The Signal-to-Noise Ratio (SNR) of the GPS signals coherently reflected over the "synthetic" lake is evaluated as a function of its radius to illustrate the contributions of higher order Fresnel zones (Fig. 3). A sudden increase in the SNR is found as the radius increases from zero to the radius of the first Fresnel zone. In the first Fresnel zone the scattered signals arrive at the receiver with a phase shift up to 90°. In the second Fresnel zone, signals subtract to the total field, since they arrive with a phase shift between 90° and 270°. In the third Fresnel zone signals add, since they arrive with a phase shift between 270° and 450°, and so on [14].

The impact of the incidence angle θ_i is strong because of the influence on the size of the Fresnel zones, the effective surface roughness, and the propagation path through the vegetation cover. Fig. 3 shows two important findings in agreement with experimental results [17]: 1) a higher coherent reflectivity for grazing angles over regions with moderate small scale surface roughness, and 2) a differentiated signal attenuation by the vegetation as a function of the incidence angle.

3.2 Validation of the GNSS-R Scattering Model

The coherent scattering model is validated using space-borne data processed with the CYGNSS raw IF processor (Fig. 4). The selected test site is a quasi-circular lake surrounded by vegetation and mountains. Several parameters were optimized so as to better capture the transition from land to the lake. In particular, the delay chip resolution was set to 1/16 chip, the Doppler resolution to 50 Hz, while the incoherent integration time was set to 10 ms using a coherent integration time of 1 ms. The nominal specular point was simulated to follow a straight trajectory across the lake, using a similar geometry and lake characteristics as those corresponding to the "real" scenario. Results show a good agreement.

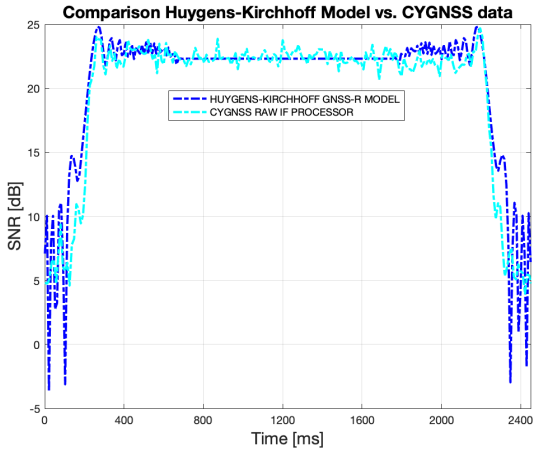

Fig. 4. Comparison of the SNR of the coherent scattering term using the Huygens-Kirchhoff GNSS-R model vs. CYGNSS raw IF space-borne data.

The model is able to capture the impact of the higher order Fresnel zones in the SNR as they are approaching the lake, and within the lake.

4. CYGNSS 2E2ES: COHERENT MODULE

The CYGNSS E2ES has been updated with the so-called "coherent module" using the electromagnetic model previously described. This module will be available for the community within the CYGNSS Science Team in a collaborative manner, so as to foster scientific studies related to the capabilities of CYGNSS for inland water body monitoring. The most relevant and useful applications will probably be for cases where there are both coherent and incoherent components to the scattered signal received by CYGNSS, and where the exact geometry of the coherently scattering surface (i.e. the boundaries of the inland water bodies) have complicated shapes.

5. CONCLUSIONS

In this work, the impact of higher order Fresnel zones on the total coherent reflected power as collected by a GNSS-R sensor is investigated over inland water bodies. The proposed model is based on the Huygens-Kirchhoff principle and it is validated using space-borne data processed with the CYGNSS raw IF processor. This model can be used to evaluate the accuracy of wetland extent retrieval algorithms over heterogenous scenes. Future research activities could also be focused on the comparison of our model with "coherent DDMs" after removing the influence of the incoherent scattering term by the computation of the variance of the coherently integrated DDMs prior to the incoherent averaging [4,13].

6. REFERENCES

[1] M. Martin-Neira, "A Passive Reflectometry and Interferometry System (PARIS): Application to Ocean Altimetry," ESA J., vol. 17, pp. 331-355, Jan. 1993.

[2] W. Li, A. Rius, F. Fabra, E. Cardellach, S. Ribo, and M. Martin-Neira, "Revisiting the GNSS-R Waveform Statistics and its Impact on Altimetric Retrievals," IEEE Transactions on Geoscience and Remote Sensing, vol. 56, no. 5, pp. 1229-1241, Jan. 2018.

[3] S.T. Lowe, J.L. LaBrecque, C. Zuffada, L.J. Romans, L.E. Young, and G.A. Hajj, "First Spaceborne Observation of an Earth-Reflected GPS signal," Radio Science, vol. 37, no. 1, pp. 7-1–7-28, Feb. 2002.

[4] H. Carreno-Luengo, "Contributions to GNSS-Reflectometry from Nano-Satellites," Ph.D. Dissertation, Dept. Signal Theory Commun., Universitat Politecnica de Catalunya, Barcelona, Spain, 2016. Online Available:https://www.tdx.cat/handle/10803/385216 (Jan. 01, 2020)

[5] S. Gleason, S. Hodgart, Y. Sun, C. Gommenginger, S. Mackin, M. Adjrad, and M. Unwin, "Detection and Processing of Bistatically Reflected GPS Signals from a Low Earth Orbit for the Purpose of Ocean Remote Sensing," IEEE Transactions on Geoscience and Remote Sensing, vol. 43, no. 6, pp. 1229-1241, Jun. 2005.

[6] M. Unwin, P. Jales, J. Tye, C. Gommenginger, G. Foti, and J. Rosello, "Spaceborne GNSS-Reflectometry on TechDemoSat-1: Early Mission Operations and Exploitation," IEEE Journal of Selected Topics in Applied Earth Observation and Remote Sensing, vol. 9, no. 10, pp. 4525-4539, Oct. 2016.

[7] H. Carreno-Luengo, S.T. Lowe, C. Zuffada, S. Esterhuizen, and S. Oveisgharan, "Spaceborne GNSS-R from the SMAP Mission: First Assessment of Polarimetric Scatterometry over Land and Cryosphere," MDPI Remote Sensing, vol. 9. no. 361, pp. 362, Apr. 2017.

[8] C. Ruf, M. Unwin, J. Dickinson, R. Rose, D. Rose, M. Vincent, and A. Lyons, "CYGNSS: Enabling the Future of Hurricane Prediction [Remote Sensing Satellites]," IEEE Geoscience and Remote Sensing Magazine, vol. 1, no. 2, pp. 52–67, Jul. 2013.

[9] C. Ruf et al., "CyGNSS Handbook. Cyclone Global Navigation Satellite System," Online Available https://clasp-research.engin.umich.edu/missions/cygnss/reference/cygnss-mission/CYGNSS_Handbook_April2016.pdf (Dec. 23, 2019)

[10] C. Ruf et al., "New Ocean Winds Satellite Mission to Probe Hurricanes and Tropical Convection," Bull. Amer. Meteorol. Soc., vol. 97, pp. 385-395, May 2015.

[11] C.D. Bussy-Virat, C. Ruf, and A.J. Ridley, "Relationship Between Temporal and Spatial Resolution for a Constellation of GNSS-R Satellites," IEEE Journal of Selected Topics in Applied Earth Observation and Remote Sensing, vol. 12, no. 1, pp. 16-25, Jan. 2019.

[12] H. Carreno-Luengo, A. Camps, I. Ramos-Perez, and A. Rius, "Experimental Evaluation of GNSS Reflectometry Altimetric Precision Using the P(Y) and C/A Signals," IEEE Journal of Selected Topics in Applied Earth Observation and Remote Sensing, vol. 7, no. 5, pp. 1493-1500, May 2014.

[13] H. Carreno-Luengo, and A, Camps, "First Dual-Band Multi-Constellation GNSS-R Scatterometry Experiment over Boreal Forests from a Stratospheric Balloon," IEEE Journal of Selected Topics in Applied Earth Observations and Remote Sensing, vol. 9, no. 10, pp. 4743-4751, Oct. 2016.

[14] H. Carreno-Luengo, and A. Camps, "Unified GNSS-R Formulation Including Coherent and Incoherent Scattering Components," in Proc. of the 2016 IEEE IGARSS, pp. 4815-4818, Beijing, China, July 2016.

[15] A. Camps, H. Park, M. Pablos, G. Foti, C. P. Gommenginger, P.-W. Liu, and J. Judge "Sensitivity of GNSS-R Spaceborne Observations to Soil Moisture and Vegetation," IEEE Journal of Selected Topics in Applied Earth Observation and Remote Sensing, vol. 9, no. 10, pp. 4730-4732, Oct. 2016.

[16] H. Carreno-Luengo, G. Luzi, and M. Crosetto, "Sensitivity of CyGNSS Bistatic Reflectivity and SMAP Microwave Brightness Temperature to Geophysical Parameters over Land Surfaces," IEEE Journal of Selected Topics in Applied Earth Observation and Remote Sensing, vol. 12, no. 1, pp. 107-122, Jan. 2019.

[17] H. Carreno-Luengo, G. Luzi, and M. Crosetto, "Above-Ground Biomass Retrieval over Tropical Forests: A Novel GNSS-R Approach with CyGNSS," MDPI Remote Sensing, vol. 12, no. 9, pp. 1368, Apr. 2020.

[18] M.-P. Clarizia, N. Pierdicca, F. Constantini, and N. Flouri, "Analysis of CyGNSS Data for Soil Moisture Retrieval," IEEE Journal of Selected Topics in Applied Earth Observation and Remote Sensing, vol. 12, no. 7, pp. 2227-2235, Jan. 2019.

[19] M. Al-Khaldi, J.T. Johnson, A.J. O'Brien, A. Balenzano, and F. Mattia, "Time-Series Retrieval of Soil Moisture Using CYGNSS," IEEE Transactions on Geoscience and Remote Sensing, vol. 57, no. 7, pp. 4322-4331, Jan. 2019.

[20] E.L. Thosos, "The Validity of the Kirchhoff Approximation for Rough Surface Scattering Using a Gaussian Roughness Spectrum," The Journal of the Acoustical Society of America, vol. 83, no. 78, pp. 78-92, Jan. 1988.

Acknowledgements

This research was supported in part by the NASA Science Mission Directorate contract NNL13AQ00C with the University of Michigan. The authors would like to thank Dr. Scott Gleason and Dr. Andrew O'Brien for their useful comments during this investigation.